GSA Data Repository 2019196

Kouketsu, Y., Tsai, C.-H., and Enami, M., 2019, Discovery of unusual metamorphic temperatures in the Yuli belt, eastern Taiwan: New interpretation of data by Raman carbonaceous material geothermometry: Geology, https://doi.org/10.1130/G45934.1

SUPPLEMENTS

Sample description

Yuli belt

Sample YL10N01 consists mainly of quartz, albite, and muscovite, with minor and accessory chlorite, tourmaline. Main constituent minerals are fine, and most quartz and albite are less than 50 μm. Crenulation cleavages are developed, which is mainly composed by micas. Black carbonaceous materials (CM) are abundantly included within the sample.

Sample F10803 is well foliated and contains quartz, phengitic muscovite, albite, chlorite, paragonite, garnet, and CM. Accessory minerals are ilmenite, rutile, titanite, epidote/allanite, tourmaline, pyrite, chalcopyrite, iron-oxide, calcite, ankerite, and zircon. Foliation is defined by interlayers of mica + chlorite and quartz. Garnet and albite are porphyroblastic but the former tends to be replaced by chlorite. Albite porphyroblasts contain inclusions of quartz, calcite, tourmaline, zircon, ilmenite, and CM, with internal foliation. Titanite is also a porphyroblatsic phase and contains quartz and carbonate inclusions.

Sample C121107 contains graphite, quartz, phengitic muscovite, paragonite, garnet, chlorite, albite, and accessory rutile, titanite, ilmenite, calcite, pyrite, tourmaline, allanite, and apatite. Two generations of phengitic muscovite can be recognized: i) intergrown with paragonite in the main foliation; ii) randomly oriented flakes as part of a retrograde assemblage. Garnet porphyroclasts, up to 2 mm in diameter, are sharply zoned with pink graphite-free cores and graphite-bearing rims. Garnet inclusions are ilmenite and quartz in the core and phengitic muscovite, chlorite, quartz, paragonite and rutile in the rim. Chlorite appears to exhibit two textures: i) porphyroblastic as part of an earlier assemblage; ii) replacing garnet and as aggregates with phengitic muscovite + quartz in the matrix as a retrograde phase. Rutile is included in garnet rims and is also a matrix mineral.

Sanbagawa metamorphic belt, southwest Japan

For the comparison of the Yuli belt, three metapelite samples collected in the Sanbagawa metamorphic belt in the Asemigawa region, central Shikoku in southwest Japan, were used. The metamorphic zonation in the Sanbagawa belt is divided to chlorite, garnet albite-biotite, and oligoclase-biotite zones from low to high grade based on the mineral assemblage of the metapelites (Enami, 1983; Higashino, 1990). In this study, representative samples from garnet zone, albite-biotite zone, and oligoclase-biotite zone were selected. The metapelitic samples in the Sanbagawa belt mainly contain quartz, albite, phengite, chlorite, epidote, CM, together with subordinated amounts of titanite, apatite, tourmaline, rutile, and zircon. The sample from the garnet zone (NSY11-24) includes garnet. The value of T_{R2} is 385-447 °C (R2 = 0.44‑0.58). The metapelite from the albite-biotite zone (NSY12-42) includes biotite. The ranges of T_{R2} is 411‑495 °C (R2 = 0.33‑0.52). The oligolcase appears in the sample from the oligoclase-biotite zone (NSY9-2) and T_{R2} is 475‑570 °C (R2 = 0.16‑0.37). The mineral assemblage and texture of the chlorite zone is similar to that of the sample YL10N01 from north edge of the Yuli belt. The metamorphic temperature of the chlorite zone of the Sanbagawa belt is usually considered at around 330 °C (Enami et al., 1994), which is the lower limit of the Raman CM geothermometer. However, despite the similarity of mineral assemblages and textures, YL10N01 collected from the northeastern edge of the Yuli belt contains mismatched high crystalline CMs.

Daimonji contact aureole, southwest Japan

The sample information of the Daimonji contact aureole of N33, N27, and N9 is described in Aoya et al. (2010). In the Daimonji area, three metamorphic zones are defined by Nakamura (1995): the chlorite, biotite, and cordierite zones, in ascending order of metamorphic temperatures based on the mineral assemblage of metapelites. N33 in the chlorite zone shows T_{R2} = <330‑422 °C (R2 = 0.49‑0.75). N27 in the biotite zone shows T_{R2}

= 461‑523 °C (R2 = 0.27‑0.40). N9 in the cordierite zone shows T_{R2} = 454‑597 °C (R2 = 0.10‑0.42).

Measurement conditions

We conducted Raman spectroscopy analyses of CM grains in the samples and estimated peak temperatures using the Raman CM geothermometer. Raman spectra of the CM were obtained using a Nicolet Almega XR (Thermo Scientific, Yokohama, Japan) with a 532 nm Nd-YAG laser passed through a confocal microscope (BX51; Olympus, Tokyo, Japan) with a 100× objective (Olympus Mplan-BD 100X, NA = 0.90). The laser power at the sample surface was set to 1–3 mW. The scattered light was collected by a backscattered geometry with a 25 μm pinhole and a holographic notch filter, dispersed using a 2400 lines/mm grating, and analyzed by a Peltier cooled CCD detector comprising 256 × 1024 pixels (Andor Technology, Belfast, Northern Ireland). The acquisition time of the CM spectra was 30 s. The spatial resolution was ~1 μm and wavenumber resolution was ~1 cm^{-1}. To avoid mechanical damage to the CM grains, we carefully selected CMs that were embedded within other transparent minerals and did not occur at the sample surface. We measured at least 30 CM grains from each sample.

Data processing

The Raman spectra of CM were decomposed into several peaks using the program PeakFit 4.12 (SeaSolve Software, Massachusetts, USA) with a pseudo-Voigt function (Gaussian–Lorentzian Sum). The spectra were corrected for the fluorescence background by subtracting a linear baseline in the spectral range of 1000–1750 cm^{-1}. The Raman spectra of CM were decomposed to the G-band (1580 cm^{-1}), D1-band (1350 cm^{-1}), and D2-band (1620

cm^{-1}). We evaluated the crystallinity of CM by using the parameter R2, which is the area ratio of D1/(G + D1 + D2), as proposed by Beyssac et al. (2002).

The parameter R2 [= $D1/(G + D1 + D2)_{area}$] decreases with increasing peak metamorphic temperature (Beyssac et al., 2002). We calculated the metamorphic temperature (T_{R2}) using the Raman CM geothermometer proposed by Beyssac et al. (2002), as follows:

$$T_{R2} = -445 \times R2 + 641. \quad (2)$$

The applicable temperature range is 330–650 °C and the error is ± 50 °C.

CM Raman spectra

Representative CM Raman spectra of maximum, average, and minimum T_{R2} for of the samples YL10N01, F10803, and C121107 are shown in Figure DR1. Every spectrum shows G-, D1-, and D2-bands excluding the D2-band of the highest T_{R2} one. Intensities of the D1- and D2-bands are highest at minimum T_{R2} spectra especially in the sample YL10N01 that shows the lowest temperature of 404 °C. The spectra showing near highest T_{R2} are likely to be detrital graphite because there are statistical outliers in F10803 and C121107.

REFERENCES CITED

Aoya, M., Kouketsu, Y., Endo, S., Shimizu, H., Mizukami, T., Nakamura, D., and Wallis, S., 2010, Extending the applicability of the Raman carbonaceous-material geothermometer using data from contact metamorphic rocks: Journal of Metamorphic Geology, v. 28, p. 895–914.

Beyssac, O., Goffe, B., Chopin, C., and Rouzaud, J.N., 2002, Raman spectra of carbonaceous material in metasediments; a new geothermometer: Journal of Metamorphic Geology, v. 20, no. 9, p. 858–871.

Enami, M., 1983, Petrology of pelitic schists in the oligoclase-biotite zone of the Sanbagawa metamorphic terrain, Japan: phase equilibria in the highest grade zone of a high-pressure intermediate type of metamorphic belt: Journal of Metamorphic Geology, v. 1, p. 141-161.

Enami, M., Wallis, S. and Banno, Y., 1994, Paragenesis of sodic pyroxene-bearing quartz schists: implications for the P-T history of the Sanbagawa belt: Contributions to Mineralogy and Petrology, v. 116, p. 182–198.

Higashino, T., 1990, The higher grade metamorphic zonation of the Sambagawa metamorphic belt in central Shikoku, Japan: Journal of Metamorphic Geology, v. 8, p. 413–23.

Nakamura, D., 1995, Comparison and interpretation of graphitization in contact and regional metamorphic rocks: The Island Arc, v. 4, p. 112–127.

FIGURE CAPTIONS

Figure DR1. Representative Raman spectra of CM in the samples YL10N01, F10803, and C121107. The top row is the spectra of the lowest T_{R2}, the middle is near the average value, and the bottom row is the spectra of the highest T_{R2}.

Fig. DR1

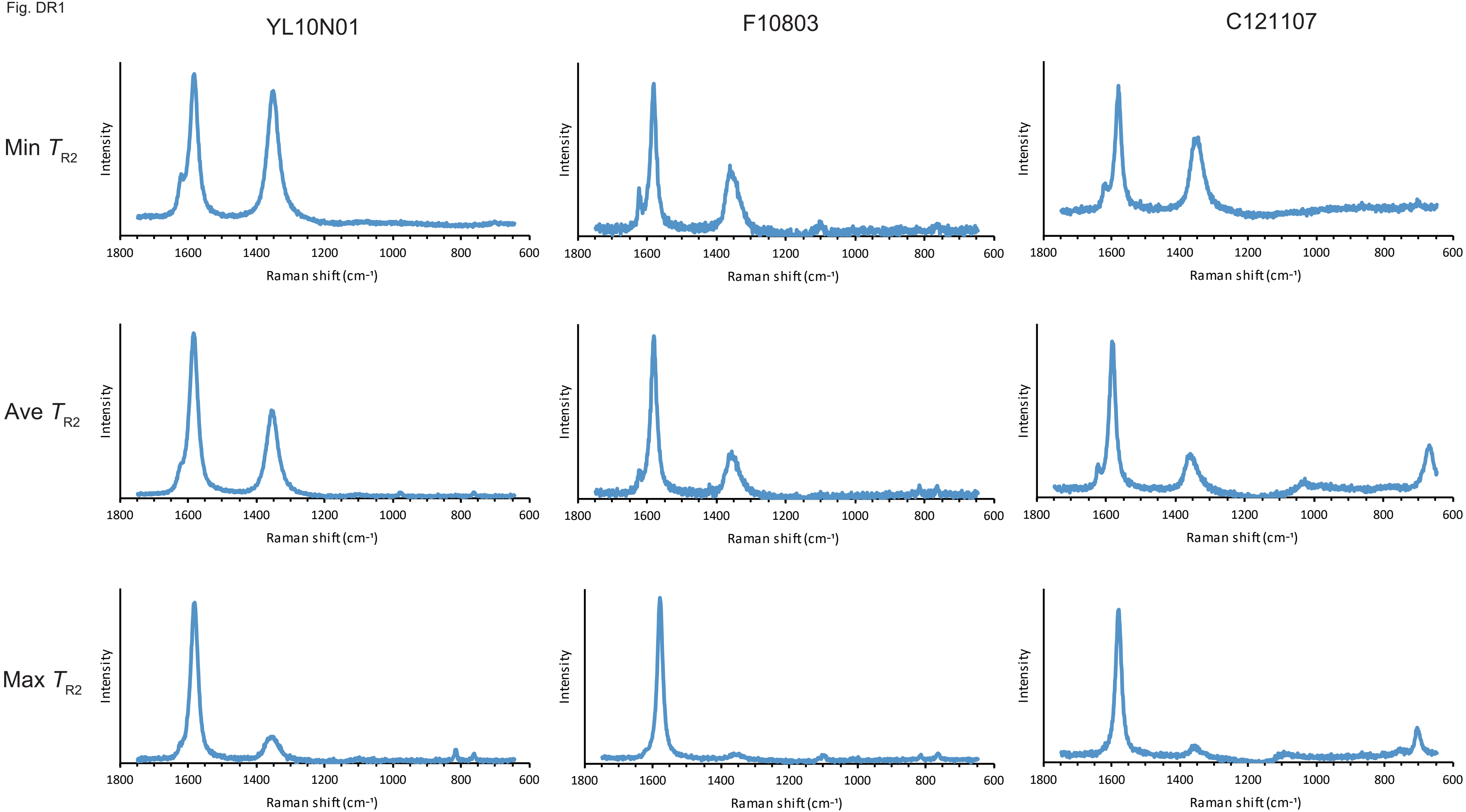
YL10N01
F10803
C121107
Min T_{R2}
Ave T_{R2}
Max T_{R2}
Intensity
Raman shift (cm⁻¹)
1800
1600
1400
1200
1000
800
600

Table DR1. Summary of CM Raman spectra data of the samples from the Yuli belt, Sanbagawa metamorphic belt, and Daimonji contact aureole.

Sample	n	R1 ratio	1σ	R2 ratio	1σ	Ave. T_{R2} (°C)	1σ (°C)
Yuli belt							
YL10N01	62	0.50	0.22	0.39	0.09	465	40
F10803	37	0.24	0.11	0.32	0.09	496	41
C121107	31	0.19	0.08	0.29	0.09	514	40
Sanbagawa belt							
NSY11-24	43	0.83	0.12	0.50	0.03	421	13
NSY12-42	34	0.52	0.12	0.42	0.04	454	19
NSY9-2	31	0.19	0.07	0.27	0.06	520	27
Daimonji							
N33	36	1.33	0.36	0.61	0.07	368	32
N27	55	0.32	0.06	0.34	0.04	491	16
N9	29	0.18	0.06	0.23	0.06	539	26

n: number of Raman spectra, R1: intensity ratio of D1- and G-bands ($[D1/G]_{Intensity}$), R2: area ratio of D1-, D2-, and G-bands ($[D1/(D1 + D2 + G)]_{Area}$), 1σ: standard deviation, Ave. T_{R2}: average T_{R2}.